The outer boundary of the hydromagnet is made of a good conductor, so that the diffusion of the field through it during the contraction period can be neglected. The field in the hydromagnet before contraction is $B_z = B_0$. Using the condition for the conservation of the flux and the field distribution (3.3) we obtain

$$B_z = B_0\left(\frac{c}{r}\right)^{\mathrm{Re}_m} \quad \frac{(\mathrm{Re}_m - 2)a^{\mathrm{Re}_m - 2}}{\mathrm{Re}_m\, c^{\mathrm{Re}_m - 2} - 2a^{\mathrm{Re}_m - 2}} .$$

It can be seen from this equation that the maximum achievable field in the center of the hydromagnet under flux-conservation conditions is $B_z = B_0(c/a)^2$ as $\mathrm{Re}_m \to \infty$. If the field on the boundary is kept constant, the field at the center of the hydromagnet is $B_z = B_0(c/a)\mathrm{Re}_m$; i.e., more effective amplification of the field occurs.

The author thanks E. I. Bichenkov and R. L. Rabinovich for useful discussions and advice.

LITERATURE CITED

1. D. A. Kleinman and A. L. Schawlow, "Corbino disk," J. Appl. Phys., 31, No. 12 (1960).
2. Ainol, Robson, and Turchi, "An interrupter based on the Hall effect for inductive circuits," Prib. Nauch. Issled., No. 4 (1977).
3. H. Kohn and O. Mawardi, "Hydromagnet: a self-generating liquid conductor electromagnet," J. Appl. Phys., 32, No. 7 (1961).
4. O. Mawardi, "Flux concentration by hydromagnetic flow," in: High Magnetic Fields, New York–London (1962).
5. V. R. Karasik, Physics and Techniques of High Magnetic Fields [in Russian], Nauka (1964).
6. M. A. Lavrent'ev and B. V. Shabat, Methods of the Theory of Functions of a Complex Variable [in Russian], Nauka, Moscow (1973).

ELECTRIC FIELDS IN A SINGLE-TURN MAGNETIC GENERATOR WITH A PARABOLIC TURN PROFILE

V. S. Fomenko

UDC 538.4

1. To solve a number of problems in experimental physics, it is necessary to have available a wide range of high-power electromagnetic energy [1]. One of the possible pulsed sources of electromagnetic energy with high specific energy capacity and power is the explosive-driven magnetic generator. Several types of explosive-driven magnetic generators are known at the present time [2-5]. The variety of generators is due to the need to satisfy contradictory requirements (e.g., such as a short operating time and a large initial inductance, a large value of the generated current, and limited dimensions of the current circuit), which are difficult to combine in a single generator.

In any type of explosive-driven magnetic generator when the condition $dL(t)/dt \gg R(t)$ is satisfied, the main increase in the generated current occurs at the end of the deformation of the electric circuit, $I(t) \sim L^{-1}(t) \cdot \eta(t)$ (I, L, and R are the current, inductance, and total resistance of the generator). The efficiency of the operation of the generator, or the value of the magnetic flux conservation coefficient η, at this stage of the magnetic-cumulative process may be reduced due to electrical breakdowns occurring in the air which fills the compression volume of the generator. The breakdown mechanism, accompanied by the cutting of part of the inductance of the circuit, and the related loss in magnetic flux, leads to considerable limitations of the electromagnet energy ($W \sim \eta^2$), and also to a reduction in the current gain ($k_T \sim \eta$), and the energy gain ($k_e \sim \eta^2$), and the fraction of the lost flux increases toward the end of the operation of the electromagnet. Increasing the coefficient η to the level specified by diffusion of the magnetic field during the compression and displacement of the flux into the generator load, is one of the main problems in constructing small-size explosive-driven magnetic generators with high output characteristics, since the technological factors (e.g., for spiral explosive-driven magnetic generators, the decentering of the spiral coil from the central tube), which affect the coefficient η, may be eliminated or reduced to a minimum. Thus, in [6] certain recommendations are made, confirmed experimentally, to achieve this purpose.

Moscow. Translated from Zhurnal Prikladnoi Mekhaniki i Tekhnicheskoi Fiziki, No. 3, pp. 49-58, May-June, 1979. Original article submitted June 15, 1978.

0021-8944/79/2003-0297$07.50

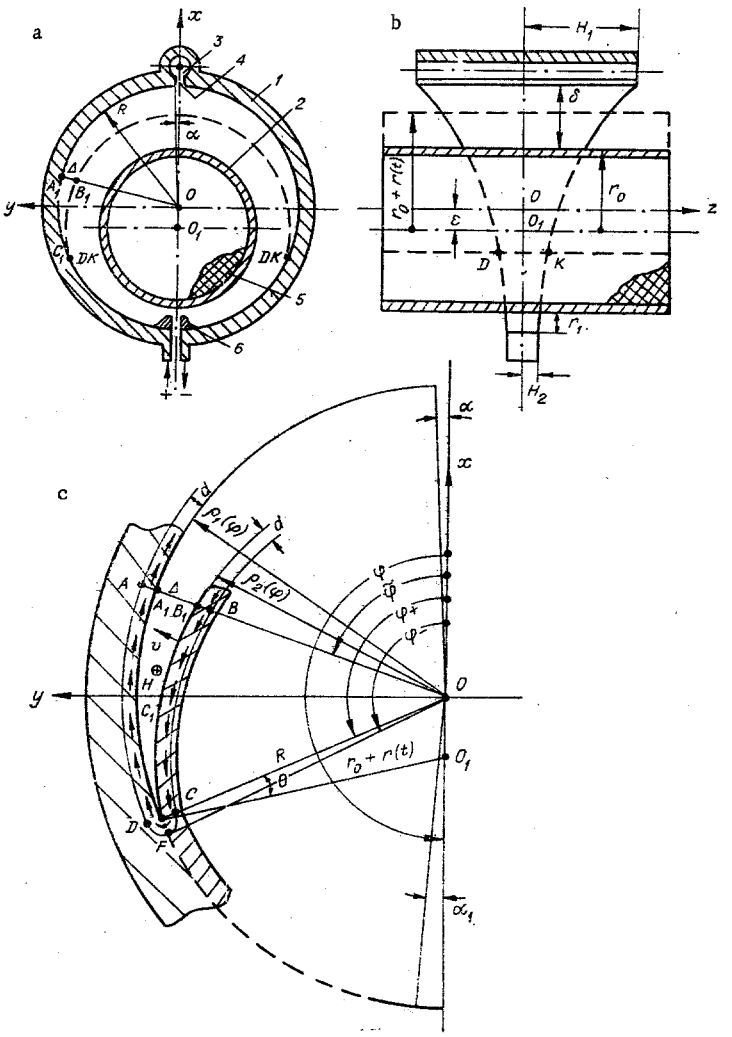

Fig. 1

One of the possible ways of increasing the operating efficiency of an explosive-driven magnetic generator is to use gases in the compression volume with higher parameters with respect to the breakdown stress than air, as was investigated in [7] for spiral and coaxial generators. However, this method does not eliminate possible loss of magnetic flux in the breakdown cutoffs in the region of the sliding (dynamic) contact of the current-carrying conductors. Thus, according to the data given in [7], it follows that the theoretical value of the coefficient η is considerably higher than the experimental value if the coefficient is calculated only taking into account the compressibility of the conductor material and the diffusion of the flux due to the finite electrical conductivity, which varies with temperature. Nevertheless an oscilloscope record of the derivative of the current from pickups placed in the current circuit of the generators contains high-frequency noise, characteristic for breakdown processes in a gas. The angle of contact of the current-carrying conductors close to the sliding contact does not exceed 0.02-0.06 rad for a magnetic field strength of 0.1-3 MOe, and in all cases experiment shows that the flux loss becomes considerable at fields exceeding 1 MOe.

A better way of increasing the operating efficiency of an explosive-driven magnetic generator is, first, to limit the growth of the magnetic field strength in the compression volume of the generator during operation to the critical value ($H(t) \leq H_*$), determined by the electrical and physical characteristics of the material of the current circuit, thus eliminating the possibility of intense electrical bursting of the skin surface of the conductors (e.g., for copper $H_* \approx 1.2$ MOe), and, second, to eliminate local electrical breakdowns in the region of the sliding contact of the conductors characteristic for magnetic generators. The first aim can be achieved by shaping the current circuit of the generator and the second by increasing the angle of contact of the conductors in the region of dynamic linking of their current-carrying surfaces. These requirements can be met most simply in a single-turn explosive-driven magnetic generator with a parabolic profile of the turn, eccentrically situated with respect to the shell of the explosive charge [8].

TABLE 1

φ_+, deg	A, cm	$\tilde{\varphi}$, deg	$H(A_1)$, MOe	$H(B_1)$, MOe	$H_+(C_1)$, MOe
180	0,2	174,26	1,256	1,257	1,257
180	0,5	165,56	1,254	1,255	1,257
180	1,0	151,02	1,214	1,237	1,257
60	0,2	52,6	1,118	1,227	1,257
60	0,5	38,84	0,939	1,05	1,257
60	0,8	15,7	0,788	0,879	1,257
65,1	1,0	0	0,697	0,767	1,257
45.26	0,5	0	0,947	0,993	1,257
28.3	0.2	0	1,126	1,147	1,257

2. Figure 1a and b shows a sketch of the generator – transverse and longitudinal sections (1, turn; 2, shell; 3, load; 4, transmission line; 5, explosive material; and 6, contact plates) with the letter notation of the dimensions employed. Figure 1c shows part of the compression volume together with the polar system of coordinates for calculating the electric field strength in a radial section of the generator at any instant of time beginning at the instant of dynamic contact of the shell with the inner surface of the winding.

For convenience we will introduce the following terminology. Generator 1 – maximum and minimum generatrices of the turn $2H_1 = 36$ cm and $2H_2 = 3$ cm, inner diameter of the turn $2R = 24.8$ cm, external diameter of the shell of explosive $2r_0 = 20.6$ cm, maximum and minimum base of flight of the shell $\delta = 3.2$ cm and $r_1 = 1$ cm, interaxial distance between the shell and the turn (eccentricity) $\varepsilon = R - r_0 - r_1 = 1.1$ cm, operating time $t_f = 12$ μsec. Generator $2 - 2H_1 = 100$-150 cm, $2H_2 = 10$-15 cm, $2R = 19.1$ cm, $2r_0 = 13.1$ cm, $\delta = 5$ cm, $r_1 = 1$ cm, $\varepsilon = 2$ cm, $t_f = 20$ μsec. Generator $3 - 2H_1 = 15$ cm, $2H_2 = 1.5$-2 cm, $2R = 19.1$ cm, $2r_0 = 13.1$ cm, $\delta = 5$ cm, $r_1 = 1$ cm, $\varepsilon = 2$ cm, $t_f = 20$ μsec.

For a closed deformed contour $\Gamma = ABCFDA$ when the magnetic flux Φ linked with it changes, we will write the law of induction with the total derivative of the flux with respect to time:

$$\oint_{\Gamma(t)} \frac{\mathbf{j}}{\sigma} d\mathbf{l} = -10^{-2} \frac{d\Phi(t)}{dt}, \tag{2.1}$$

where

$$\frac{\mathbf{j}}{\sigma} = \mathbf{E}^* = \mathbf{E} + 10^{-2}[\mathbf{v}(t)\,\mathbf{B}]; \quad \Phi(t) = \int_{S_\Gamma(t)} \mathbf{B}[z(\rho, \varphi), t]\, d\mathbf{s}, \; t, \; \mu\text{sec},$$

where the electric field strength $\mathbf{E}$ satisfies the law of induction in partial derivatives of Φ with respect to t:

$$\oint_{\Gamma} \mathbf{E} d\mathbf{l} = -10^{-2} \frac{\partial \Phi(t)}{\partial t}\Big|_{v=0,\ B \neq \text{const}};$$

v(t) is the velocity of flight of the shell due to the action of the products of the explosion and the back pressure of the magnetic field.

In the region of the sliding contact between the shell and the winding $\rho_{B\breve{C}F}(\varphi) \leqslant \rho(\varphi) \leqslant \rho_{A\breve{D}F}(\varphi), \tilde{\varphi}(t) \leq \varphi \leq \varphi_-(t)$, the distribution of the magnetic induction B can be assumed to be close to uniform and to vary only slightly with time during the operation of the generator, since the nature of the variation (increase) of the generatrix of the winding $z(\rho_1, \varphi)$ along the path of displacement of the magnetic flux in the load is close to the law of the amplitude growth of the current. This means that along unit length of the line $DK = z[\rho_1, \varphi_+(t)]$ (see Fig. 1b) there is a constant value of the current $\left(j_+(t) = \frac{B_+(t)}{0.4\pi\mu_1} \approx \text{const}\right)$, which with a corresponding choice of the initial magnetic flux Φ_0 and the final induction L_f which is not higher than the critical value

$$j_* = \frac{4 \cdot 10^4}{\pi\mu_1}\left(\frac{c_V D}{\varkappa} T_*\right)^{1/2} \gtrsim j_+(t) = \frac{\eta(t)\,\Phi_0}{[L(t) + L_f]} \frac{1}{z[\rho_1, \varphi_+(t)]},$$

where c_V, D, and T_* are the specific heat, J/g·deg, the density, g/cm^3, and the melting point of the material of the conductors, respectively, and $\varkappa$ is a coefficient which depends on the shape and duration of the field; e.g., for an exponential increase it is 2/3 [9].

The results of a calculation of the induction B at the points A_1, B_1, and C_1 are shown in Table 1 for several fixed positions of the shell φ_+ and for different values of the gap between the shell and the turn $A_1B_1=\Delta$, for a linear current density along the line DK of 1 MA/cm, close to the critical value for copper conductors. The data in Table 1 relate to generators 2 and 3.

Then, assuming that the induction B on the surface of the conductors and in the skin layer are equal, we can represent the left side of Eq. (2.1) in the form

$$\oint\limits_{\Gamma(t)} \frac{\mathbf{j}}{\sigma}\, d\mathbf{l} = E_1^*(t)\,[\Delta(t) + 2d(t)] + \int\limits_{\Gamma_1(t)} \frac{\mathbf{j}}{\sigma}\, d\mathbf{l}, \tag{2.2}$$

where

$$\int\limits_{\Gamma_1(t)} \frac{\mathbf{j}}{\sigma}\, d\mathbf{l} \approx \langle j\rangle \frac{1}{\langle\sigma\rangle} l_{\Gamma_1}(t) \leqslant \frac{j_+}{\sigma_+} \frac{l_{\Gamma_1}(t)}{d(t)}$$

with

$$\langle j\rangle = \frac{\langle B\rangle}{0{,}4\pi\mu_1 d(t)} \leqslant \frac{j_+}{d(t)}, \quad \langle\sigma\rangle = \sigma_0(1 + k_0\langle T\rangle)^{-1} \leqslant \sigma_+ = \sigma_0(1 + k_0 T_+)^{-1},$$
$$l_{\Gamma_1}(t) = l_{\breve{BC}}(t) + l_{\breve{AD}}(t) + \pi d(t),$$

and

$$\langle j\rangle = \frac{1}{3}[j(A_1) + j(B_1) + j_+(C_1)], \quad \langle B\rangle = \frac{1}{3}[B(A_1) + B(B_1) + B_+(C_1)].$$

If $j_+=j_*$, then $\sigma_+=\sigma_*$, $T_+=T_*$. Thus, for copper conductors $\sigma_*\approx 10^5\ \Omega^{-1}\cdot\mathrm{cm}^{-1}$ and $T_*\approx 10^3$°C. Here Γ_1 is the contour BCFDA; d, skin depth; μ_1, relative magnetic permeability; $l_{\breve{BC}}$ and $l_{\breve{AD}}$, length of the arcs BC and AD, respectively; k_0, temperature coefficient of the electrical resistance; σ, conductivity; and E_1^*, electric field strength in the region of the line of dynamic contact between the shell and the turn.

From (2.1) and (2.2), provided that in the region of the sliding contact $S_\Gamma(t)\frac{d}{dt}\langle B\rangle \ll \frac{dS_\Gamma(t)}{dt}\langle B\rangle$, we obtain

$$E_1^*(t) = -\frac{\langle H\rangle}{\Delta(t) + 2d(t)}\left[\frac{l_{\Gamma 1}(t)}{0{,}4\pi d(t)\langle\sigma\rangle} + 10^{-2}\frac{dS_\Gamma(t)}{dt}\right]. \tag{2.3}$$

Here

$$\Delta(t) = R + \varepsilon\cos\tilde{\varphi}(t) - [r_{01}^2 u^2[\varphi_+(t)] - \varepsilon^2\sin^2\tilde{\varphi}(t)]^{1/2}, \tag{2.4}$$

where

$$u[\varphi_+(t)] = \frac{r_0 + r(t)}{r_{01}} = \left\{1 + 4p\cos^2\left[\frac{1}{2}\varphi_+(t)\right]\right\}^{1/2},$$

whence we obtain the following expression used below:

$$\dot{\varphi}_+(t) = -\frac{v(t)\, r_{01} u[\varphi_+(t)]}{R\varepsilon\sin\varphi_+(t)}\ \dagger \tag{2.5}$$

with

$$r_{01} = r_0 + r_1, \quad p = \frac{R\varepsilon}{r_{01}^2}.$$

By considering the triangle OC_1O_1 we obtain the angle of contact of the expanding shell with the inner surface of the turn,

$$\theta[\varphi_+(t)] = \arcsin\left\{\frac{\varepsilon\sin\varphi_+(t)}{r_{01}u[\varphi_+(t)]}\right\}, \tag{2.6}$$

which varies during the generator operation, and its numerical value is determined by the dimensions of the transverse cross section of the current-carrying elements (the shell and the turn) of the generator and their eccentricity ε, while (2.5) and (2.6) are connected by the relation

† Here and later the dot above a quantity denotes differentiation with respect to time t.

$$\dot{\varphi}_+ t = -\frac{v(t)}{R\sin\theta[\varphi_+(t)]}.$$

Introducing the approximations $l_{\widetilde{BC}}(t) \approx l_{\widetilde{AD}}(t) \approx l_{\widetilde{A_1C_1}}(t) = R[\varphi_+(t) - \widetilde{\varphi}(t)]$, $v = \text{const}$, $d = \text{const}$, $S_\Gamma(t) \approx S_{\Gamma_2}(t) + 2dR[\varphi_+(t) - \widetilde{\varphi}(t)] + \frac{\pi}{2}d^2$, where Γ_2 is the contour $A_1B_1C_1A_1$, and calculating the area $S_{\Gamma_2}(t)$ in polar coordinates with the pole at the point O using the equations of the inner boundary of the turn and the external boundary of the shell, which respectively have the form

$$\rho_1(\varphi) = R, \quad \rho_2(\varphi) = \{r_{01}^2 u^2[\varphi_+(t)] - \varepsilon^2\sin^2\varphi\}^{1/2} - \varepsilon\cos\varphi,$$

after differentiating $S_{\Gamma_2}(t)$ with respect to time, we obtain

$$\begin{aligned}\frac{d}{dt}S_\Gamma(t) = \frac{1}{2}\Big\{&\left[R^2 + 4Rd - r_{01}^2u^2(\varphi_+(t))\right]\dot{\xi}(t) - 2vr_{01}u[\varphi_+(t)]\xi(t)\\ &+ \varepsilon^2[u_2(t)\dot{\varphi}_+(t) - \dot{\widetilde{u}}_2(t)\widetilde{\varphi}(t) + u_3(t)] + 2vr_{01}u[\varphi_+(t)][\theta(\varphi_+(t))\\ &- \arcsin\left(\frac{\varepsilon}{r_{01}}\frac{\sin\widetilde{\varphi}(t)}{u(\varphi_+(t))}\right)\Big] + r_{01}^2u^2[\varphi_+(t)][u_4(t) - \widetilde{u}_4(t)]\Big\},\end{aligned} \tag{2.7}$$

where

$$u_2(t) = u_1(t)\cos\varphi_+(t) - \cos 2\varphi_+(t); \quad \widetilde{u}_2(t) = \widetilde{u}_1(t)\cos\widetilde{\varphi}(t) - \cos 2\widetilde{\varphi}(t);$$

$$u_3(t) = \dot{u}_1(t)\sin\varphi_+(t) - \dot{\widetilde{u}}_1(t)\sin\widetilde{\varphi}(t); \quad \xi(t) = \varphi_+(t) - \widetilde{\varphi}(t);$$

$$u_4(t) = \frac{1}{u_1(t)}\left\{\dot{\varphi}_+(t)\cos\varphi_+(t) - \frac{v\sin\varphi_+(t)}{r_{01}u[\varphi_+(t)]}\right\}; \quad \widetilde{u}_4(t) = \frac{1}{\widetilde{u}_1(t)}\left\{\dot{\widetilde{\varphi}}(t)\cos\widetilde{\varphi}(t) - \frac{v\sin\widetilde{\varphi}(t)}{r_{01}u[\varphi_+(t)]}\right\};$$

$$u_1(t) = \{p_1u^2[\varphi_+(t)] - \sin^2\varphi_+(t)\}^{1/2}, \quad \widetilde{u}_1(t) = \{p_1u^2[\varphi_+(t)] - \sin^2\widetilde{\varphi}(t)\}^{1/2},$$

with

$$\dot{u}_1(t) = v\frac{R - \varepsilon\cos\varphi_+(t)}{R\varepsilon\cos\theta[\varphi_+(t)]}, \quad \dot{\widetilde{u}}_1(t) = \frac{2p_1\frac{v}{r_{01}}u[\varphi_+(t)] - \dot{\widetilde{\varphi}}(t)\sin 2\widetilde{\varphi}(t)}{2\widetilde{u}_1(t)}, \quad p_1 = \frac{r_{01}^2}{\varepsilon^2}.$$

Case 1. For a fixed angle $\widetilde{\varphi}(t) = \text{const}$, $(\dot{\widetilde{\varphi}}(t) = 0$ in (2.7)) and for a running variable $\varphi_+(t)$ $(\dot{\varphi}_+(t) \neq 0)$, which varies over the range of values $\widetilde{\varphi} \leq \varphi_+(t) < \pi$, we can evaluate (2.3) in the radial section AO of the compression volume, when $\Delta(t)$ decreases $(\Delta(t) \to 0, \dot{\Delta}(t) \neq 0)$ during the generator operation.

Case 2. We can calculate the electric field strength $E_1^*(t)$ as a function of $\varphi_+(t)$ $(\dot{\varphi}_+(t) \neq 0)$ for a fixed value of the gap $\Delta(t) = \Delta = \text{const}$ $(\dot{\Delta}(t) = 0)$ if we know the quantity $\dot{\widetilde{\varphi}}(t) \neq 0$ in (2.7).

For the second case we have from (2.4)

$$\widetilde{\varphi}(t) = \arccos\left\{\frac{r_{01}^2u^2[\varphi_+(t)] - \varepsilon^2 - p_2^2}{2\varepsilon p_2}\right\},$$

whence it follows that

$$\dot{\widetilde{\varphi}}(t) = -\frac{r_{01}u[\varphi_+(t)]}{\varepsilon p_2}v\left\{1 - \left[\frac{r_{01}^2u^2(\varphi_+(t)) - \varepsilon^2 - p_2^2}{2\varepsilon p_2}\right]^2\right\}^{-\frac{1}{2}},$$

and furthermore, the running variable $\varphi_+(t)$ is bounded by the range of values $\varphi_1 \leq \varphi_+(t) < \pi$, where

$$\varphi_1 = 2\arccos\left[\frac{(p_2 + \varepsilon)^2 - r_{01}^2}{4R\varepsilon}\right]^{\frac{1}{2}} + \alpha$$

with

$$p_2 = R - \Delta.$$

3. The results of a numerical calculation using Eq. (2.6) are shown in Fig. 2a for generators 1 and 2 (curves 1 and 2, respectively), having the same value of the minimum base of flight of the shell $r_1 = 1$ cm. Data for a similar calculation of $\theta(\varphi_+)$ for generator 3 are shown in Fig. 2b. Curves 1-6 correspond to $r_1 = 0$ (3 cm), 0.5 cm (2.5 cm), 1 cm (2 cm), 1.5 cm (1.5 cm), 2 cm (1 cm), and 2.5 cm (0.5 cm). The values of the interaxial distances of the shell and the turn are shown in brackets.

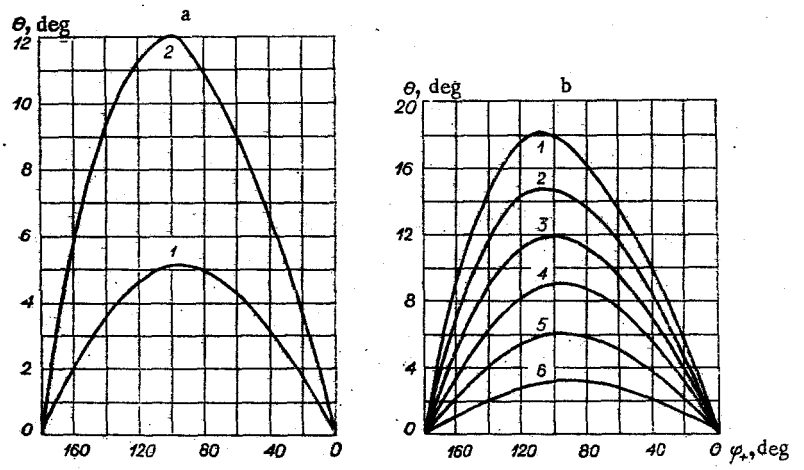
θ, deg
a
12
10
8
6
4
2
0
160
120
80
40
0
2
1
θ, deg
b
20
16
12
8
4
0
160
120
80
40
0
φ+, deg
1
2
3
4
5
6

Fig. 2

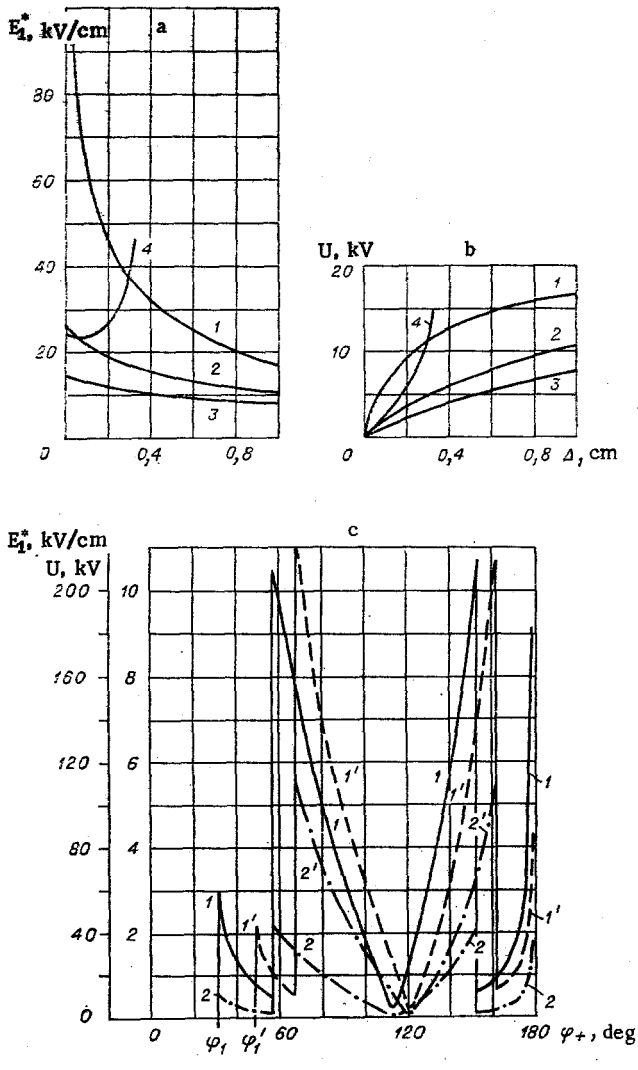
E1*, kV/cm
a
80
60
40
20
0
0,4
0,8
4
1
2
3
U, kV
b
20
10
0
0,4
0,8
Δ, cm
c
E1*, kV/cm
U, kV
200
160
120
80
40
0
10
8
6
4
2
60
120
180
φ+, deg
φ1
φ1'
1'
2'

Fig. 3

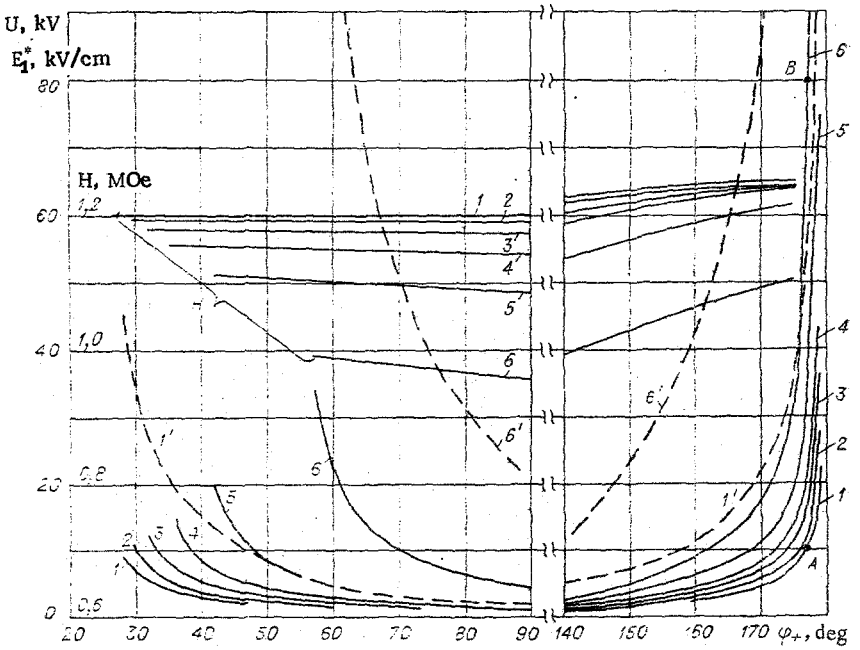

Fig. 4

It follows from the theoretical data shown in Fig. 2 that in generators with the same value of r_1 the angle θ depends on the geometrical dimensions (diameters) of the turn and the shell. When the eccentricity ε is reduced (when r_1 is increased) the angle θ decreases, which leads to an increase in the electric field strength in the region of the sliding contact. In addition, the angle θ has a larger value at the beginning of the dynamic contact between the shell and the turn than at the end of the generator operation (see the verticals $\varphi_+ = 20°$ and 160° in Fig. 2b).

The results of a calculation of the electric field strength E_1^* and the voltage $U = \Delta E_1^*$ for generator 2 as a function of the distance between the shell and the turn $\Delta(\tilde{\varphi}, t)$ are shown in Fig. 3a and b, in the form of curves 1-4, respectively, for different fixed values of $\tilde{\varphi}$ ($\alpha = 2.5$; 40; 90; 150°), for a linear current density of 1 MA/cm along the line DK. The maximum value E_1^* occurs in the final stage of the generator operation (curve 1, Fig. 3a, $\tilde{\varphi} = \alpha = 2.5°$) and does not exceed a value of 90 kV/cm for $\Delta = 0.04$ cm. Figure 3c shows graphs of E_1^* and U as a function of φ_+ for fixed Δ, and in the region of variation $60° \leqslant \varphi_+ \leqslant 160°$ the amplitude values of the quantities are measured along the ordinate axis with increased scale (curves 1 and 2 – E_1^*, U for $\Delta = 0.2$ cm, and curves 1', 2' – E_1^*, U for $\Delta = 0.5$ cm). The large values of E_1^* which occur at the beginning of the dynamic contact between the shell and the turn ($\varphi_+ \approx 180°$), are easily eliminated by introducing contact plates into the generator construction (see Fig. 1a position 6), which shift the beginning of the contact elements of the generator into the range of values $\varphi_+ = 180° - \alpha_1$ (in Fig. 3c the results of the calculation correspond to $\alpha_1 = 1°$, $\alpha \leqslant 4°$).

The variation in the voltage in the compression volume of the generator 3 close to the sliding contact ($\Delta = 0.2$ cm) as a function of φ_+ ($\varphi_1 \leq \varphi_+(t) \leq \pi - \alpha_1$, $\alpha \leqslant 3$-4°, $\alpha_1 = 1°$) for different values of the eccentricity ε (3, 2.5, 2, 1.5, 1, 0.5 cm) is shown in Fig. 4 in the form of graphs 1-6, respectively. Curves of U (1-6 in Fig. 4) also correspond to curves of $\theta(\varphi_+)$ (1-6 in Fig. 2b). The curves of the electric field strength 1' and 6' correspond to the outermost curves 1 and 6 of the voltage. The values of the magnetic field strength (curves of the field H 1-6 correspond to curves U 1-6) in the region of the sliding contact were averaged as $[H(A_1) + H(B_1) + H_+(C_1)]/3$ for a linear current density of 1 MA/cm along the line DK.

The calculated data in Fig. 4 confirm the considerable increase in the electric field strength in the region of the sliding contact (by a factor of 5-8 in the initial stages of the contact between the shell and the turn) when the eccentricity ε is reduced from 3 cm to 0.5 cm (points A and B in Fig. 4). The values of the electric field for a relative position of the shell and the turn close to coaxial ($\varepsilon = 0.5$ cm) facilitate the development of local electric breakdowns in the region of the sliding contact (curve 6'). This is confirmed by the presence of intense luminescence of the air in this region, recorded in experiments with an almost coaxial position of the shell and the turn ($\varepsilon \approx 0.2$ cm), and also by the absence of luminescence when the interaxial distance is increased to values $\varepsilon \geqslant 1$ cm for the same magnetic field strength ~1 MOe.

The values of the eccentricity $\varepsilon \geqslant 1$ cm for an overall thickness of the insulating film of 0.2-0.4 mm placed on the inner surface of the turn, the transmission line, and the load, enables electrical breakdown to be eliminated in the region of the sliding contact during the whole magnetic-cumulative process for generators 1-3 when operating with a constant linear current density of ~1 MA/cm along the line of contact of the conductors.

Calculations using (2.3) were carried out for a value of the shell velocity $v = 0.25$ cm/μsec, equal to the average experimental value. The value of the skin depth, according to data given in [9], is 0.03 cm for a duration of the exponentially growing current pulse of ~16 μsec, equal to the operating time of generators 2 and 3 at the stage of contact between the shell and the inner surface of the turn. The value of the electrical conductivity was taken for copper conductors at the melting point, viz., $\sigma_* = 10^5\ \Omega^{-1} \cdot \text{cm}^{-1}$.

4. The initial inductance of the profiled turn generator, unlike the unprofiled turn generator, depends on the interaxial distance between the shell and the turn, and the inductance increases and the time of generator operation decreases as ε is reduced. The rate of variation of the inductance reaches a maximum value when $\varepsilon = 0$. However, the choice of the value of ε is determined first of all by the possible reduction in the loss in magnetic flux in the region of dynamic linking between the current-carrying surfaces of the shell and the turn, the reason for which is local electrical breakdown. By an appropriate choice of the dimensions of the transverse cross section of the shell and the turn, and also of their mutual position (i.e., by choosing the eccentricity), one can obtain values of E_1^* which practically eliminate the possibility of electrical breakdowns in the region of the sliding contact between the current-carrying conductors under critical field-strength conditions ($H \approx H_*$) for a thickness of the insulating layer, which has no effect on the ohmic resistance of the contacting conductors.

LITERATURE CITED

1. Physics of High Energy Density, Proceedings of the International School of Physics, Academic Press, New York–London (1971).
2. A. D. Sakharov et al., "Magnetic cumulation," Dokl. Akad. Nauk SSSR, 165, No. 1 (1965).
3. S. J. Lukasik, G. W. Zerko, and R. L. Jameson, "Magnetic flux compression in an explosion geometry," Proc. Conf. Megagauss Magnetic Field Generation by Explosives and Related Experiments, Frascati, Italy (1965), Brussels Eur. Atom (1966), pp. 367-386.
4. F. Herlach and H. Knöpfel, "Megagauss fields generated in explosive-driven flux compression devices," Rev. Sci. Instrum., 36, No. 8 (1965).
5. E. I. Bichenkov, "Explosive-driven generators," Dokl. Akad. Nauk SSSR, 174, No. 4 (1967).
6. A. D. Sakharov, "Explosive-driven magnetic generators," Usp. Fiz. Nauk, 88, No. 4 (1966).
7. J. W. Shearer et al., "Explosive-driven magnetic field compression generators," J. Appl. Phys., 39, No. 4 (1968).
8. A. Ya. Koshelev, V. S. Fomenko, and V. I. Chizhov, "Explosive-driven current generator," Byull. Izobret., No. 33 (1974).
9. H. Knöpfel, Pulsed High Magnetic Fields, North-Holland, London (1970).